Earthquake Engineering, Tenth World Conference © 1992 Balkema, Rotterdam. ISBN 90 5410 060 5

Seismic response analysis for jointed buried pipeline by using shell FEM model

S.Takada
Kobe University, Japan

S.Higashi
Sekisui Chemical Industry Ltd, Shiga, Japan

ABSTRACT: This paper presents a shell model FEM formulation of jointed buried pipelines and results of their numerical calculations. An elastic thin shell theory was used for an analysis in which the shell was supported by non-linear axial, circumferential and radial soil springs. The axial and circumferential springs were uniformly distributed in strength around the shell surface, but the distribution of radial soil spring depends on the transversal movement of pipelines. The present paper introduces a new technique to analyse responses of the shell with an arbitrary distribution of the radial soil springs. Seismic wave propagation and dislocation of ground were assumed as input forces for the shell pipeline. It was found that the stress of the pipelines has been reduced considerably due to the effects of joints and that deformations in the cross section of the pipe are an important factor for large diameter pipelines.

1 SHELL MODEL AND ANALYSING THEORY

1.1 *Matrix displacement method for* shell analysis

It is well known in a thin shell theory that if loadings are functions of sine or cosine along the circumference, the responses are also distributed in the same way along that directions. Thus, it is only necessary to consider an amplitude in the analysis. For an asymmetric case , the loading is expanded into Fourier series and then responses are calculated to each Fourier term (Sticklin et al.,1968, Kameda et al. ,1988). We could obtained responses by superposing the calculated results. In Fig.1 an arbitrary element eij in the cylindrical coordinate that was employed in the analyses is illustrated. The generalized displacements and forces of an arbitrary nodal circle i are given by Eq.(1).

$$\{d_i\} = [u_i, v_i, w_i, \beta_i]^T$$
$$\{f_i\} = [Q_i, T_i, H_i, M_i]^T \qquad (1)$$

Where ui, vi and wi are displacements in axial, circumferential and radial directions respectively. Vi,Ti and Hi are corresponding forces in those directions. Mi and βi are the moment and rotation angle tangent to the nodal circle. The generalized nodal forces and displacements corresponding to arbitrary expanded terms in the loading Fourier series are expressed in the following.

$$\{d_i\} = [u_{in}(x)\mathrm{Cos}n\theta, v_{in}(x)\mathrm{Sin}n\theta, w_{in}(x)\mathrm{Cos}n\theta, \beta_{in}(x)\mathrm{Cos}n\theta]^T \qquad (2)$$

$$\{f_i\} = [Q_{in}(x)\mathrm{Cos}n\theta, T_{in}(x)\mathrm{Sin}n\theta, H_{in}(x)\mathrm{Cos}n\theta, M_{in}(x)\mathrm{Cos}n\theta]^T \qquad (3)$$

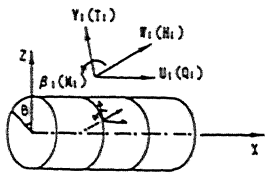

Fig.1 Elements in generalized coordinate System

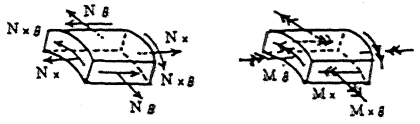

Fig.2 Directions of generalized forces in an element

Displacements in the element eij can be shown as

$$\{u_n\} = [u_n(x), v_n(x), w_n(x), \beta_n(x)]^T \quad (4)$$

Assuming the displacement to be a polynomial function in the axial coordinate, that is

$$\{u_n\} = \begin{bmatrix} 1 & \xi & 0 & 0 & 0 & 0 & 0 & 0 \\ 0 & 0 & 1 & \xi & 0 & 0 & 0 & 0 \\ 0 & 0 & 0 & 0 & 1 & \xi & \xi^2 & \xi^3 \\ 0 & 0 & 0 & 0 & 0 & 1/L & 2\xi/L & 3\xi^2/L \end{bmatrix} \cdot \begin{Bmatrix} a_1 \\ a_2 \\ \vdots \\ a_8 \end{Bmatrix} \quad (5)$$

Where $\xi = s/L$ is a dimensionless axial coordinate, and s is a distance from nodal circle i to the circle considered. Substitute boundary conditions into Eq.(5) and coefficient am, m=1,2,....,8 can be calculated. Then the generalized displacements are given by

$$\{u_n\} = [N]\ \{d_{ijn}\} \quad (6)$$

The strain of the arbitrary surface are easily obtained as

$$\{\varepsilon_n\} = [B]\ \{d_{ijn}\} \quad (7)$$

in which [B] is a 6*8 matrix . The directions of forces in an element are shown in Fig.2. The forces can be written as

$$\{\sigma_n\} = [N_{xn}, N\theta_n, N_x\theta_n, M_{xn}, M\theta_n, M_x\theta_n]^T \quad (8)$$

The generalized Hook's law here becomes

$$\{\sigma_n\} = [D]\ \{\varepsilon_n\} \quad (9)$$

We have next equations by using the virtual displacements principle for an element eij assuming that inertia and damping effects are negligible.

$$-\int_\theta^{2\pi}\int_\theta^L \delta\{\varepsilon\}^T\{\sigma\}rdsd\theta + \int_\theta^{2\pi}\delta\{d_{ij}\}^T\{f_{ij}\}rd\theta + \int_\theta^{2\pi}\int_\theta^L \delta\{u\}^T\{p\}rdsd\theta = 0 \quad (10)$$

Eq.(10) can be simplified as

$$-\int_\theta^L \delta\{\varepsilon_n\}^T\{\sigma\}ds + \delta\{d_{ijn}\}^T\{f_{ijn}\} + \int_\theta^L \delta\{u_n\}^T\{p_n\}ds = 0 \quad (11)$$

(2) Shell model with non-uniform circumferential distribution of radial soil spring

Fig.3 shows a shell model used for this analysis. As can be seen a thin shell model is supported by three kinds of soil springs. It is supported by the axial and circumferential shear springs which are distributed uniformly on the shell surface. But the radial spring is distributed non-uniformly on it because it causes the difference by the pipeline's action of pulling or compression forces. In short, there exist no or very small pulling forces between pipes and ground. Thus, radial earth pressure is distributed like as shown in Fig.4. The earth pressure is neglected in the part of pipeline surface which catch pulling force. To consider this distribution, radial springs are assumed to be non-symmetrically distributed(see Fig.5). Friction forces per unit length associated with relative displacement are illustrated in Fig.6. Soil springs are assumed to be bi-linear as shown in the figure. By using the Hooke's law, earth pressure is written as

$$\{p_n\} = \begin{Bmatrix} p_{xn} \\ p\theta_n \\ p_{zn} \\ p\beta_n \end{Bmatrix} = \begin{cases} k_x(U_n - u_n) \\ k\theta(V_n - v_n) \\ k'_z(W_n - w_n) \\ 0 \end{cases} \quad (12)$$

Where

$$k'_z = \begin{cases} 0 & \cdots\cdots W - w > 0 \\ k_z & \cdots\cdots W - w < 0 \end{cases} \quad (13)$$

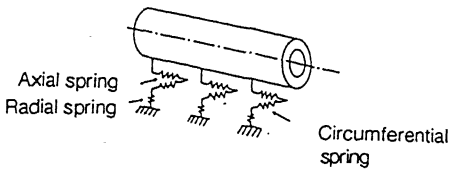

Fig.3 Ground-pipeline system in shell model

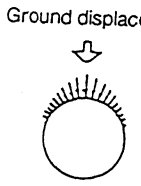

Fig.4 Actual radial earth-pressure

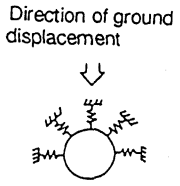

Fig.5 Distribution of radial spring corresponding to shell model

Consider the ground movement downwards first, kz' being rewritten as

$$k'_z = \begin{cases} 0 & \cdots\cdots \pi/2 < \theta < 3\pi/2 \\ k_z & \cdots\cdots -\pi/2 < \theta < \pi/2 \end{cases} \quad (14)$$

Thus the radial earth pressure can be rewritten as

$$P_z = [W_s(x) - w_s(x)]\ k'_z\cos\theta \quad (15)$$

where $kz'\cos\theta$ is distributed same as in Eq.(13), so it can readily be approximated by finite Fourier series as

$$k'_z \cos\theta = k_z \{ 1/\pi + \cos\theta/2 + (-1)^{k+1} 2/\pi \cdot \Sigma \cos 2k\theta/(4k^2-1) \} \quad (16)$$

Considering the harmonic number merely up to 2k=10, we could obtain a good approximation. By substituting Eqs.(6),(7),(9) and (12) in Eq.(11), the resulting equation comes out to be as followings

$$\{f_{ijn}\} + \{P_n\} = ([K_n] + [K_s])\{d_{ijn}\} \quad (17)$$

In which [Kn] is a stiffness matrix of the pipeline. It is quite difficult to calculate [Kn] by direct integration, but it can readily be evaluated by numerical integration. [Ks] is the stiffness matrix due to the soil springs. {fijn} is the nodal force vector, {Pn} is the loading vector.

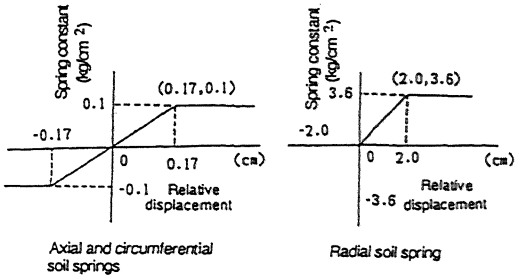

Fig.6 Soil springs related with relative displacements

(3) Joint elements, global relations and boundary conditions

Goodman's joint elements were considered as shown in Fig.7. The technique is that forces of the joint element are calculated from relative displacement at the both ends of the shell elements. The relative displacement vector is expressed as Eq.(18) in which nodal displacements are used.

$$\{u_{\theta n}\} = [L_\theta]\{d_{ijn}\} \quad (18)$$

A stiffness matrix [C] connects the forces of the joint element with the nodal displacements .

$$\{f_{ijn}\} = [C]\{u_{\theta n}\} = [C][L_\theta]\{d_{ijn}\} = [K_j]\{d_{ijn}\} \quad (19)$$

We multiply both sides of Eq.(19) by [λ] and integrate it from 0 to 2πas shown in Eq.(20).

$$\sum_{n=0}^{1} \int_0^{2\pi} [\lambda^n]^T [\lambda^n] r\, d\theta \{f_{ijn}\} = \sum_{n=0}^{1} \int_0^{2\pi} [\lambda^n]^T [K_j] [\lambda^n] r\, d\theta \{d_{ijn}\}$$

$$[\lambda^n] = \mathrm{diag}[\cos n\theta, \sin n\theta, \cos n\theta, \cos n\theta, \cos n\theta, \sin n\theta, \cos n\theta, \cos n\theta] \quad (20)$$

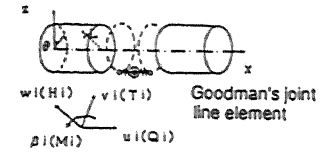

Fig.7 Shell elements and joint element in generalized coordinate system

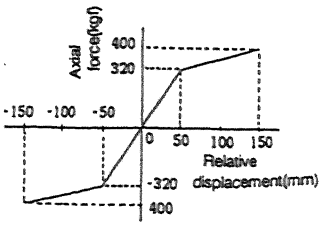

Fig.8 Axial force related with relative displacement of joint element

By assuming Eq.(17) corresponding to all elements, we have a global relation by putting Eq.(20) in it. One example of the joint character is shown in Fig.8.

1.2 CALCULATED RESULTS AND DISCUSSION

(1) Response calculations under SV wave

Response values of a jointed or continuous pipeline subjected to SV wave with an amplitude of 2.5 cm, 100m wave length and an incident angle of zero degree to the x direction are presented in Figs.9-14 along the stretch of the pipeline. Dimensions of buried pipeline used for calculations are shown in Table 1. Response values of axial stress in the jointed pipeline by shell theory is known to be smaller than those by beam theory as shown in Fig.9. Axial stress for the continuous pipeline shows almost same value between two analytical methods. Fig.10 is the distribution of pipe displacement along the pipeline which shows the pipeline follows ground movement when it has mechanical joints. Fig.11 is a distribution of radial displacement of the pipe section. The radial displacement by shell theory is smaller than those by beam theory and the radial displacement in compression area in ground motions is larger than tension area due to non-uniform

distribution of soil springs. Figs.12 and 13 show distributions of soil spring constants in axial and radial directions at the final step of numerical calculations by the loading incremental method. The section where soil spring shows small value corresponds to slip areas between pipe and ground. Fig.14 is distributions of pipe rotation along pipeline. The figure indicates that bending of pipe itself is relieved by joint characters.

Table 1 Dimension of FRPM

Diameter(mm)	800	Pipe length(cm)	500
Thickness(mm)	20	Young's Modulus (kgf/cm²)	90,000
Cross area(mm²)	5314		
Moment of inertia(mm⁴)	12.6	Poison's ratio	0.2

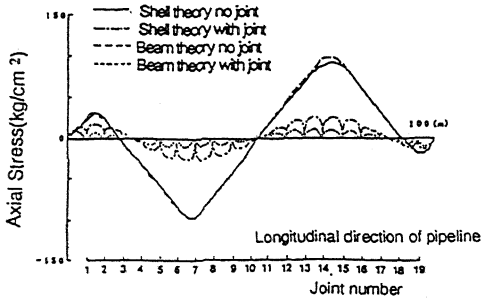

Fig.9 Distribution of axial stress at pipe crown along pipeline

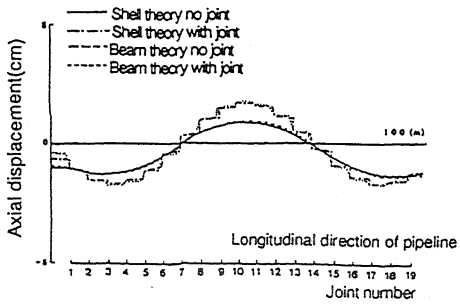

Fig.10 Distribution of axial deformation along pipeline

(2) Response calculations under ground dislocation

Figs.15-21 are distributions of response of the buried jointed or continuous pipelines with same dimensions as mentioned above when it is subjected to ground dislocation such as fault movements at center position of the pipeline with an amplitude of 5 cm and a dip angle of 45 degrees. Axial stress both in jointed and continuous pipelines by shell model is much smaller than those by beam theory as shown in Fig.15. Fig.16 is

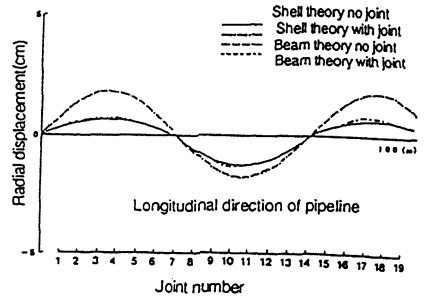

Fig.11 Distribution of radial displacement along pipeline

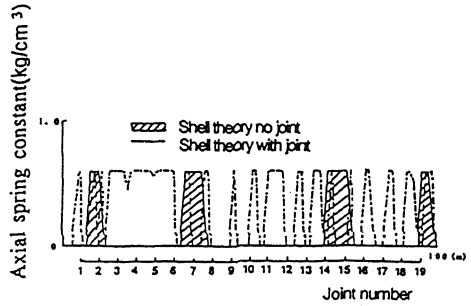

Fig.12 Distribution of axial spring constant along pipeline

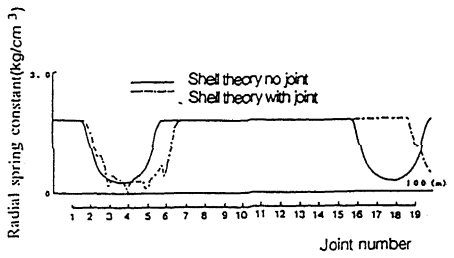

Fig.13 Distribution of radial spring constant along pipeline

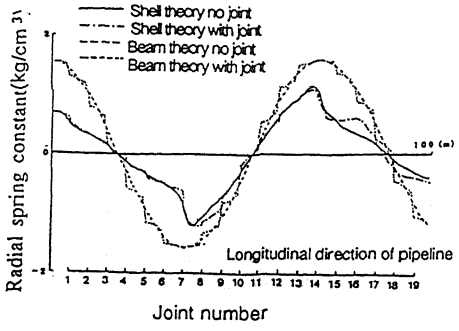

Fig.14 Distribution of rotation angle along pipeline

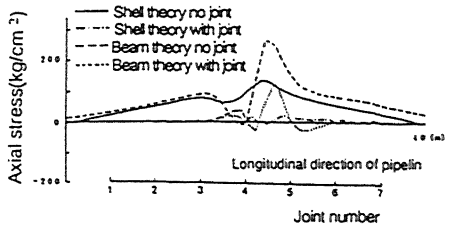

Fig.15 Distribution of axial stress at pipe crown along pipeline

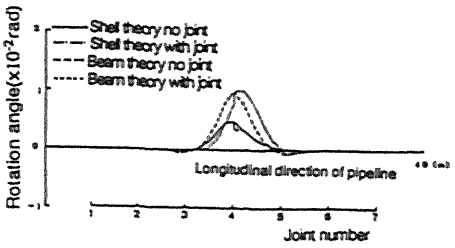

Fig.19 Distribution of rotation angle along pipeline

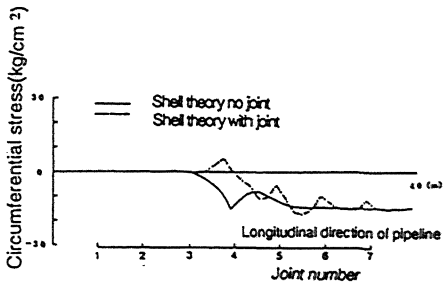

Fig.16 Distribution of circumferential stress at pipe crown along pipeline

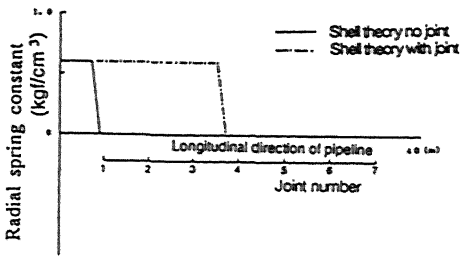

Fig.20 Distribution of axial spring constant along pipeline

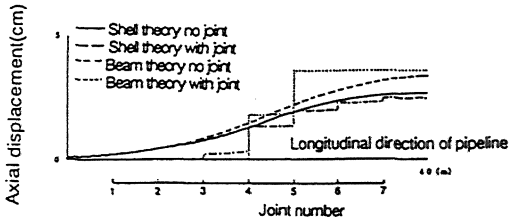

Fig.17 Distribution of axial deformation along pipeline

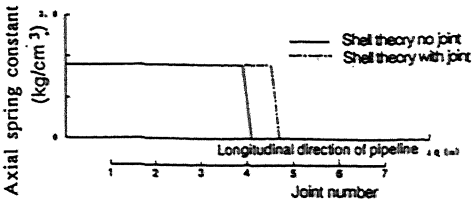

Fig.21 Distribution of radial spring constant along pipeline

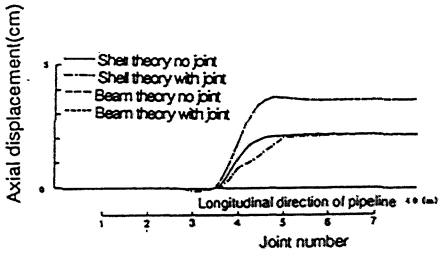

Fig.18 Distribution of radial displacement along pipeline

the distribution of circumferential stress which can not be obtained by beam theory. The value of the circumferential stress can not be negligible compared with axial stress. Figs.17 and 18 are distributions of axial and radial pipe displacements along pipelines respectively. The difference of the pipe displacement calculated by shell or beam theory is distinct in the radial displacement due to consideration of non-uniform distribution of soil spring. Rotation of pipe elements is shown in Fig.19. Distributions of soil spring constants are shown in Figs.20 and 21 for axial and radial directions. More slippage can be seen in axial direction compared with radial ones.

1.3 CONCLUSIONS

Present paper treats seismic response analytical method for a buried jointed or continuous pipeline with relatively large diameter by using thin shell theory. Numerical calculations were performed for Φ800mm FRPM buried pipelines when it is subjected to seismic wave and/or ground dislocation and results were compared with ones by beam theory.

(1) A computer program has been developed for the response calculation of buried jointed or continuous pipeline subjected to seismic wave and/or ground dislocation by using a thin shell theory.
(2) The present shell model can calculates the distortion of cross section of pipeline and circumferential stress which could not be obtained by beam theory. Further, the shell model can take account of the distribution of real earth pressure around the cross section of pipes.
(3) Jointed pipelines can absorb ground deformations much more than continuous pipelines indicating that the jointing is one of the effective countermeasures under seismic environments.

REFERENCES

Kameda,H., S.Takada and R.Yang,1988. Shell model FEM analysis of buried pipelines under seismic loading, Bull.Disa.Res.Inst.,Kyoto Univ.,Vol.38, No.3:115-146.

Sticklin,J.A.,W.E.Haisler,H.R.McDougall and F.J.Stebbins ,1968. Nonlinear analysis of shell of revolution by the displacement method,AIAA, Journal Vol.6, No.12:2306-2312.